Brain Structure and Function (2020) 225:1055–1071
https://doi.org/10.1007/s00429-020-02058-x

ORIGINAL ARTICLE

Ex vivo diffusion-weighted MRI tractography of the Göttingen minipig limbic system

Johannes Bech[1] · Dariusz Orlowski[1] · Andreas N. Glud[1] · Tim B. Dyrby[2,3] · Jens Christian H. Sørensen[1] · Carsten R. Bjarkam[4]

Received: 25 September 2019 / Accepted: 18 March 2020 / Published online: 3 April 2020

Abstract

The limbic system encompasses a collection of brain areas primarily involved in higher cognitive and emotional processing. Altered function in the limbic circuitry may play a major role in various psychiatric disorders. This study aims to provide a high-quality ex vivo diffusion-weighted MRI (DWI) tractographic overview of the Göttingen minipig limbic system pathways, which are currently not well described. This may facilitate future translational large animal studies. The study used previously obtained post-mortem DWI scans in 3 female Göttingen minipigs aging 11–15 months. The tractography performed on the DWI data set was made using a probabilistic algorithm, and regions of interest (ROIs) were defined in accordance with a histological atlas. The investigated pathways included the fornix, mammillothalamic tract, stria terminalis, stria medullaris, habenulo-interpeduncular tract, and cingulum. All the investigated limbic connections could be visualized with a high detail yielding a comprehensive three-dimensional overview, which was emphasized by the inclusion of video material. The minipig limbic system pathways displayed using tractography closely resembled what was previously described in both human studies and neuronal tracing studies from other mammalian species. We encountered well-known inherent methodological challenges of tractography, e.g., partial volume effects and complex white matter regions, which may have contributed to derouted false-positive streamlines and the failure to visualize some of the minor limbic pathway ramifications. This underlines the importance of preexisting anatomical knowledge. Conclusively, we have, for the first time, provided an overview and substantial insight of the Göttingen minipig limbic system.

Keywords Cingulum · Fornix · Mammillothalamic tract · Stria medullaris · Stria terminalis · Sus scrofa

Introduction

The limbic system has been subjected to great interest as well as puzzlement, since Paul Broca described "le grand lobe limbique" (Broca 1877). The strive to understand and identify the primary brain areas responsible for emotions and higher cognition continued with Papez' circuit of emotion (Papez 1937) and the later studies of Yakovlev (1948) and Maclean (1949, 1952). From an evolutionary perspective at that time, however , a segregation of cognition and emotion was present with the latter being deemed a more primitive trait that could be ascribed to the limbic system, whereas more intellectual functions of mammalian species were related to the neocortical areas (LeDoux 2000). Since then, the concept has evolved further; however, there is currently no broad scientific consensus on which brain structures constitute the limbic system, and some have even discussed if the term should be abandoned (Kotter and

Electronic supplementary material The online version of this article (https://doi.org/10.1007/s00429-020-02058-x) contains supplementary material, which is available to authorized users.

✉ Johannes Bech
jb@clin.au.dk

1 CENSE, Department of Neurosurgery, Department of Clinical Medicine, Aarhus University Hospital, Aarhus University, Palle Juul-Jensens Boulevard 165, Entrance J, 8200 Aarhus N, Denmark

2 Danish Research Centre for Magnetic Resonance, Center for Functional and Diagnostic Imaging and Research, Copenhagen University Hospital Hvidovre, 2650 Hvidovre, Denmark

3 Department of Applied Mathematics and Computer Science, Technical University of Denmark, 2800 Kongens Lyngby, Denmark

4 Department of Neurosurgery, Department of Clinical Medicine, Aalborg University Hospital, 9100 Aalborg, Denmark

Stephan 1997). However, neuroscientific research is increasingly continuing to both explore and understand the neuronal circuitry and mechanisms underlying, e.g., memory, spatial orientation, emotion, fear, reward, and various psychiatric conditions related to limbic brain areas (Catani et al. 2013; Murray 2007; Mayberg 1997; LeDoux 2000; Aggleton and Brown 1999; Seo et al. 2018; Gomes et al. 2018). Thus, treatment-resistant depression has been linked to a pathological activity within limbic–cortical circuits, previously modulated using deep-brain stimulation (DBS) of the subgenual cingulate white matter (Mayberg et al. 2005). Likewise, a pathological information flow between the amygdala and the accumbens nucleus has been suggested to be involved in anxiety disorders and obsessive–compulsive disorder (OCD), also potentially treatable with DBS (Sturm et al. 2003; Huff et al. 2010). Other white matter abnormalities have been observed in patients suffering from bipolar disorder or schizophrenia, where tractography disclosed altered connectivity in the anterior thalamic projections and the uncinate fasciculus (McIntosh et al. 2008). Another white matter structure, the habenulo-interpeduncular pathway (fasciculus retroflexus), has been linked to nicotine addiction (Antolin-Fontes et al. 2015). These examples indicate the importance and relevance of understanding the pathological mechanisms involving limbic structures. To this end, translational studies are generally valuable, since they permit the use of invasive methods, various research setups, and post-mortem analyses (Glud et al. 2011; Sorensen et al. 2011). To perform such studies, it is, however, a prerequisite to have the sufficient prior anatomical understanding.

The Göttingen minipig is an excellent candidate for translational large animal models due to several factors. It has a human-resembling physiology, and a relatively large gyrencephalic brain relative to its body size, which still permits the use of clinical surgical equipment as well as clinical scanners (Bjarkam et al. 2008; Lind et al. 2007; Fang et al. 2012; Dolezalova et al. 2014; Orlowski et al. 2017). Moreover, the minipig is easily handled and can be trained for both neurologic testing and behavioral analyses (Glud et al. 2010; Christensen et al. 2018; Lillethorup et al. 2018), and it is a more economical and ethically feasible animal model than non-human primates (Bjarkam et al. 2009; Sorensen et al. 2011). The neuroanatomical insight and histological knowledge of the minipig have increased over the recent years, and several structures and features are already well described including the telencephalon (Bjarkam et al. 2017a), the accumbens nucleus (Meidahl et al. 2016), the corticospinal tract (Bech et al. 2018), and the hypothalamus (Ettrup et al. 2010), as well as central cholinergic structures (Mahady et al. 2017) and prefrontal cortex and connections (Jelsing et al. 2006). The limbic system, on the other hand, yet remains somewhat poorly understood in the Göttingen minipig hindering potential translational studies in this animal.

Tractography, derived from diffusion-weighted magnetic resonance imaging (DWI), is a non-invasive method used to investigate white matter structures and connectivity within the brain. It exploits the anisotropic diffusion of water molecules in biological tissues that provide insight to the underlying white matter anatomy (Basser et al. 1994). Previously, tractography has been used in human studies of limbic white matter tracts, but has been reported to suffer from low resolution and partial volume effects (Concha et al. 2005; Kamali et al. 2016), where the latter results from different tissue properties averaged within one voxel. As this can reduce the anisotropy within, for instance, the juxtaventricular voxels, streamlines may terminate prematurely. The use of ex vivo DWI has, however, yielded high-quality data (Dyrby et al. 2011) with a higher resolution than can normally be obtained in human clinical settings and an advantageous signal-to-noise ratio. Moreover, current advanced models have addressed the previous issues with resolving fibers that traverse complex white matter regions using multi-fiber reconstruction methods and probabilistic algorithms (Tournier et al. 2010, 2012; Behrens et al. 2007), and tractography has achieved great accordance with the "gold standard" method of displaying neuronal connectivity, i.e., invasive neuronal tracing (Bech et al. 2018), although recently it has been discussed if invasive neuronal tracing is becoming more of a "silver standard" (Dyrby et al. 2018) with new emerging techniques.

This study aims to investigate and describe the neuroanatomy of the major pathways within the Göttingen minipig limbic system by the use of high-quality ex vivo tractography. These limbic system pathways have not yet been well described in the minipig to the authors' best knowledge. We hope to provide a new anatomical insight in this animal. Our data will be compared with previous neuronal tracing data from other species for evaluation. Moreover, we wish to provide a spatially comprehendable three-dimensional overview of this system's anatomy through the inclusion of video material. Such spatial understanding may otherwise be difficult to obtain merely through viewing two-dimensional histological sections. In doing this, we wish to make the connectivity within this complex system easier to recognize. By increasing the neuroanatomical knowledge of the minipig limbic system, we hope to facilitate future translational studies on the limbic circuitry in health and disease in porcine large animal models.

Materials and methods

Our study used scans previously obtained (Bech et al. 2018). Details are written below under the respective sections.

Animals

This study used three female Göttingen minipigs (Ellegaard Göttingen Minipigs, Dalmose, DK), JBG3–5, aging 11–15 months and weighing 22.6–28.0 kg, as approved by the Danish National Council of Animal Research Ethics (protocol number 2015-15-0201–00965).

Tissue fixation

The animals were transcardially perfusion-fixated using phosphate-buffered paraformaldehyde (PFA) in a 4% solution as previously described (Ettrup et al. 2011; Bech et al. 2018). The brains with upper spinal cords were removed (Bjarkam et al. 2017b) and the tissue was placed in a 4% PFA solution before being transferred to a neutral 0.01 M phosphate-buffered solution at least a week prior to DWI scanning.

Image acquisition

The ex vivo diffusion-weighted MRI scans were performed at the Danish Research Centre for Magnetic Resonance (DRCMR) on a 4.7 T Agilent MR scanner. The scans were made using a pulsed-gradient spin-echo sequence (PGSE) with a single line readout. A DWI data set included nine $b = 0$ s/mm^2 and a b value of 6500 s/mm^2 ($\delta = 7$ ms, $\Delta = 20$ ms, gradient strength = 320 mT/m) acquired in 128 non-collinear directions (Jones 2004). Voxel size was $0.5 \times 0.5 \times 0.5$ mm^3 and 105 slices ensured whole brain coverage (TR = 7200 ms, TE = 35 ms). Scanning time was approximately 48 h per session.

Tractography

Tractography of the respective limbic tracts were performed with MRtrix 3 software (https://www.mrtrix.org) (Tournier et al. 2012). In FSL software (https://fsl.fmrib.ox.ac.uk/fsl/fslwiki/FSL) (Jenkinson et al. 2012), a brain mask was made by drawing an ROI on the b0 image in 'fslview' to confine the analyses to the actual brain tissue. Next, a multi-fiber reconstruction method, i.e., constrained spherical deconvolution, was used in MRtrix 3 Software (Tournier et al. 2004, 2007). Tractography was performed using the probabilistic algorithm, iFOD2 (Tournier et al. 2010). White matter regions of interest (ROIs) were placed within the respective investigated tracts and used for streamline seeding. These seeding ROIs were manually defined based on the combination of an existing histological minipig atlas (Bjarkam et al. 2017a; Orlowski et al. 2019), along with a priori neuroanatomical knowledge and orientation distribution function (ODF) glyphs in 'mrview' of the MRtrix software package (Tournier et al. 2012), see Fig. 1. Since the standard streamline tractography parameters apply mainly to an in vivo setting, these were empirically adjusted to the ex vivo data set as described below, where the individual seeding strategies are also described. Generally, a relatively high fractional anisotropy (FA) cut-off was chosen to reduce the number of false positives, although resulting in immediate termination of streamlines when entering gray matter regions. Accordingly, the streamlines do not propagate to different gray matter anatomical subregions and, hence, only display white matter connections between larger gray matter regions. The angle between successive steps in streamline propagation was experimentally found not to alter the results and was kept in a standard setting. The number of generated streamlines was 10,000 in all tractographies as is commonly done in other studies (Liptrot et al. 2014). Tractography was performed bilaterally in all animals. The cut-off for individual connections is summarized in Table 1 along with the use of either inclusion ROIs acting as waypoints for streamline propagation and/or exclusion ROIs, where such were deemed to reliably exclude obvious false negatives as is described in the following. The respective tractography data were displayed with the diffusion tensor imaging (DTI) FA image as a background, which was made in the FSL software (https://fsl.fmrib.ox.ac.uk/fsl/fslwiki/FSL) (Jenkinson et al. 2012).

Fornix

A seeding ROI was placed at the column of the fornix (see Fig. 1a) using bidirectional tracking allowing the streamlines to propagate from a readily identifiable point in the rostral fornix, which was yet centered enough to avoid previously described issues of path-length dependency confounds introduced with longer streamline routes in probabilistic algorithms (Liptrot et al. 2014). Moreover, this position allowed streamlines to divide into the expected ventral pre- and postcommissural subdivisions of the fornix (Kamali et al. 2015) without the allowance of large angles in streamline propagation, which could potentially bias the results. Exclusion ROIs were used close to the midsagittal plane of the fornix to display only the unilateral projections in the tractography. This obviously also hindered the commissural connections, e.g., the hippocampal commissure, in being represented, but was necessary to produce a realistic and anatomically plausible distribution of the fornix. Furthermore, an exclusion ROI was placed at the respective optic tracts, since their position, close to the white matter boundary of the hippocampi, produced false-positive streamlines continuing in the optic tracts.

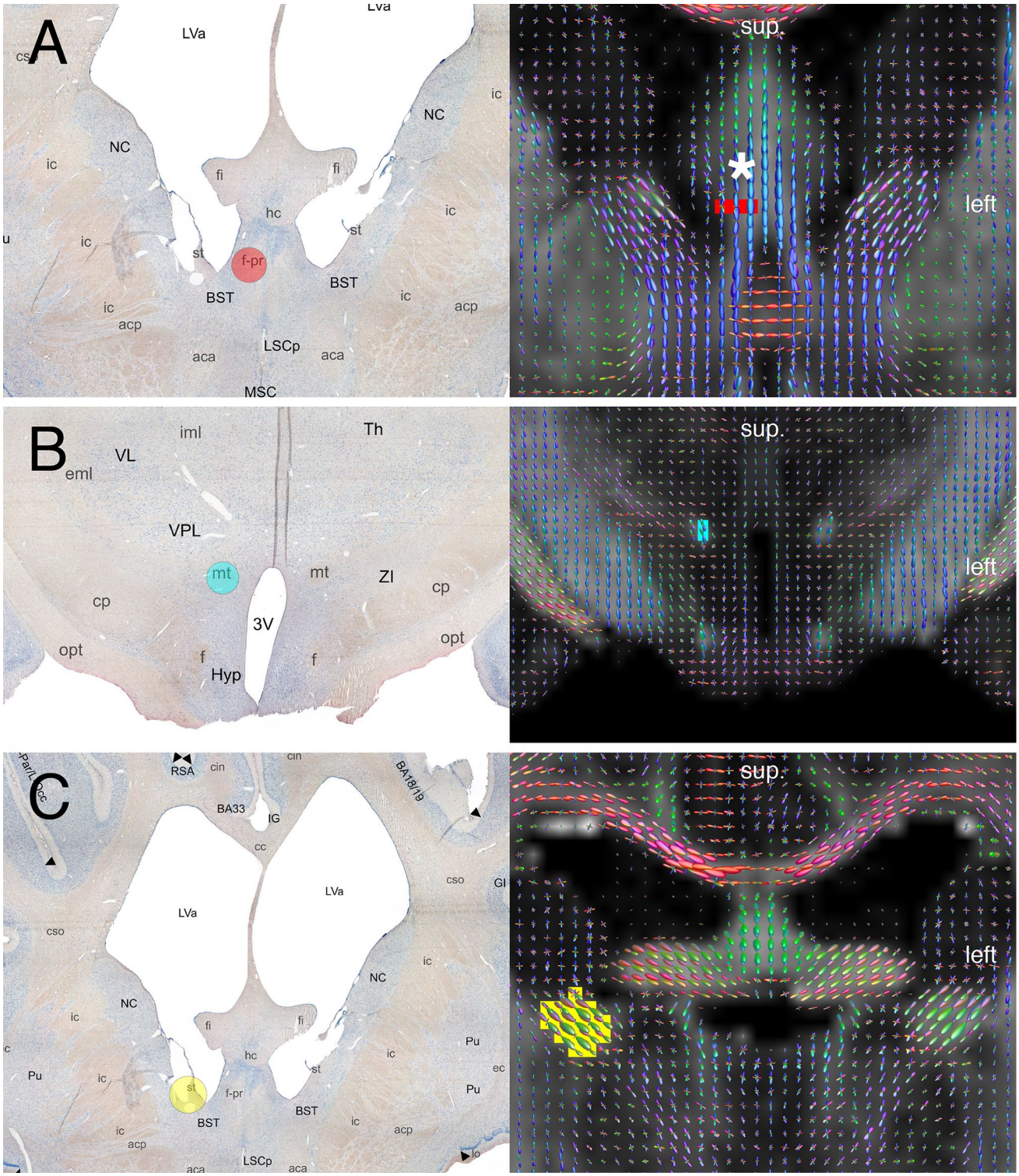

Fig. 1 The figure display the seeding ROIs used for tractography supported by the use of a histological atlas of the Göttingen minipig brain (Bjarkam et al. 2017a; Orlowski et al. 2019). Left are the histology images with colored circles illustrating the correspondingly colored seeding ROIs on DWI images to the right, which also displays overlaying ODF glyphs. Row **a** is the fornix (note the asterisk indicating that this ROI was in the axial plane), (f-pr) precommisural fornix. Row **b–d** shows the mammillothalamic tract (mt), stria terminalis (st), and stria medullaris (sm). Row **e** illustrates the habenulo-interpeduncular tract (fasciculus retroflexus, fr). The double asterix indicates that the upper green circle was not directly used for ROI placement, since it was difficult to histologically identify the tract in this region. The lower green circle outlines the contralateral "fr" marking on the histology image. On the DTI image, the corresponding area is seen to be a part of the white matter tract constituting the left habenulo-interpeduncular tract, see also text. Row **f** displays the dorsal cingulum (cin). The remaining seeding ROIs of the cingulum are displayed in the supplementary

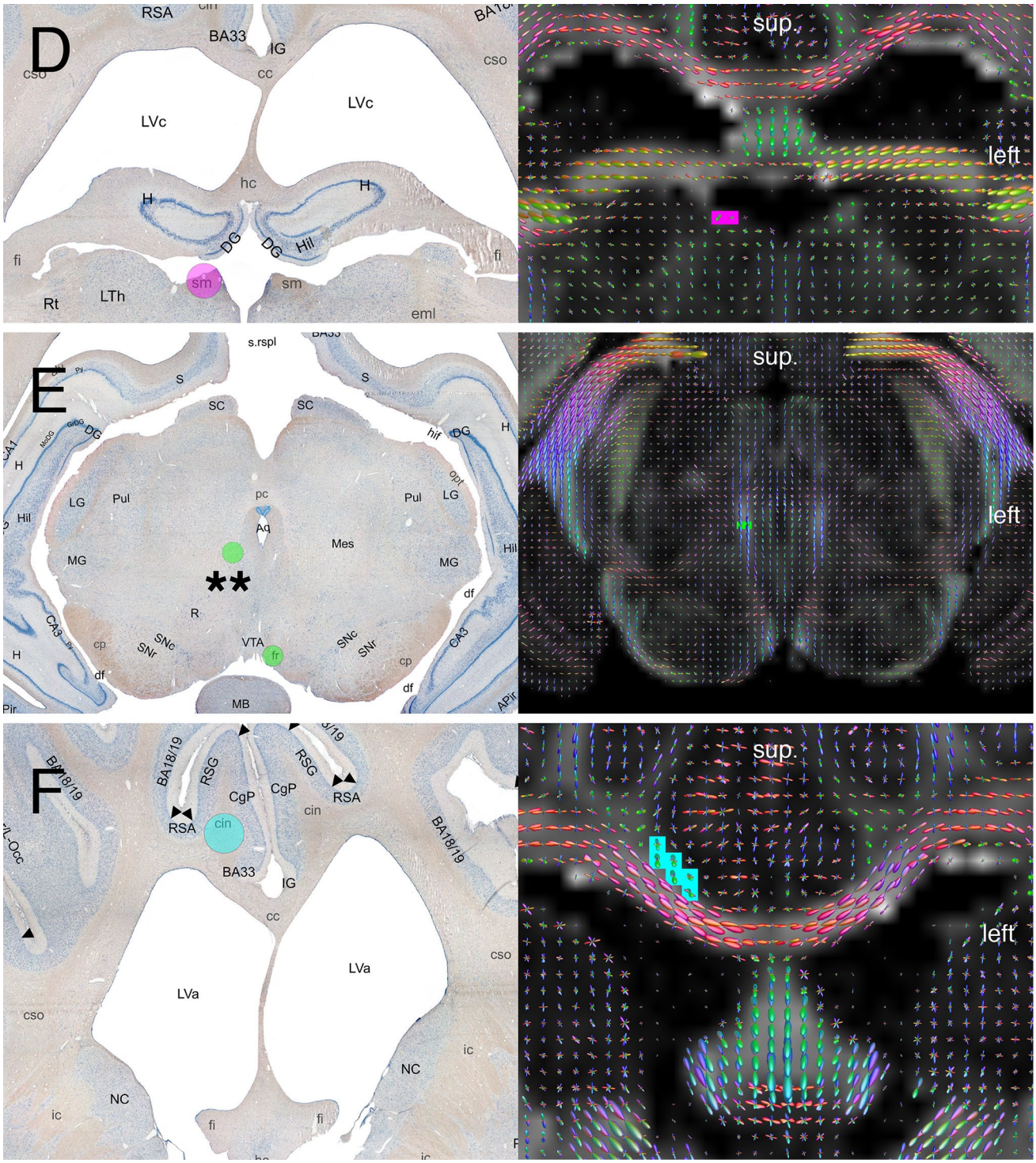

Fig. 1 (continued)

The mammillothalamic tract (bundle of Vicq d'Azyr)

Due to the well-defined part of the mammillothalamic (MT) fiber bundle that is ventrally located in the diencephalon, the seeding ROI was placed here (see Fig. 1b) with bidirectional streamline propagation. The high FA value, well over 0.3 within the voxels containing this bundle, permitted a relatively high FA cut-off value of 0.25. This high cut-off value also avoided the presence of likely false positives in the lower anisotropy voxels adjacent to the seeding ROI. No

Table 1 Tractography parameters of the individual limbic tracts

Animal no	JBG3/4/5
Fornix	
Cut-off	0.275 (0.3[†])
Inclusion ROIs	No
Exclusion ROIs	Yes
Mammillothalamic tract	
Cut-off	0.25
Inclusion ROIs	No (Yes[‡])
Exclusion ROIs	No
Stria terminalis	
Cut-off	0.3
Inclusion ROIs	No
Exclusion ROIs	Yes
Stria medullaris	
Cut-off	0.3
Inclusion ROIs	No
Exclusion ROIs	Yes
Habenulo-interpeduncular tract	
Cut-off	0.275
Inclusion ROIs	No
Exclusion ROIs	No
Dorsal cingulum	
Cut-off	0.25
Inclusion ROIs	Yes
Exclusion ROIs	No
Anterior cingulum	
Cut-off	0.25
Inclusion ROIs	Yes
Exclusion ROIs	Yes
Temporal cingulum	
Cut-off	0.25
Inclusion ROIs	Yes
Exclusion ROIs	Yes

Cut-off is FA cut-off and the remaining rows state if inclusion or exclusion ROIs were used for the individual tractographies. See text for details

[†]JBG5 had a cut-off of 0.3

[‡]JBG5 had an inclusion ROI as waypoint (see supplementary Fig. 2b)

waypoints were needed in JBG3/4, but an inclusion waypoint ROI was used in JBG5, see supplementary Fig. 2b.

Stria terminalis

The distinct position of the stria terminalis (ST) bundle, where it is situated between the superiorly located caudate nucleus and the inferiorly located anterior thalamus, was manually defined as seeding ROI (see Fig. 1c). This site was chosen for two reasons, first of which was to start propagation of streamlines in a position with high anisotropy and not in immediate relation to the complex white matter areas along the route of the ST. Second, this position would address possible path-length dependency confounds described above. Exclusion ROIs were placed at the anterior commissure, optic tracts and fornix, since these massive fiber bundles are distributed in near proximity to the ST and otherwise forced streamlines to falsely continue here. In one animal (JBG 4), streamlines progressed through the complex white matter area of the centrum semiovale to then cross the midline at the posterior corpus callosum, where an exclusion ROI was also placed here in this animal.

Stria medullaris

The seeding ROI was placed at the highly anisotropic small medial region at the vertex of the diencephalon below the fimbria–fornix, where the stria medullaris (SM) is also well defined histologically (Bjarkam et al. 2017a) (see Fig. 1D). An exclusion ROI was used to avoid streamlines continuing with the postcommissural fornix fibers, see supplementary Fig. 4b. No inclusion ROIs were needed.

The habenulo-interpeduncular tract (fasciculus retroflexus)

The midpoint of this tract was difficult to identify in the histology atlas (Bjarkam et al. 2017a) due to its superior–inferior direction parallel to the coronal section planes. On the axial view of the FA image, a small well-defined area displayed high anisotropy and ODF glyphs indicated a superior–inferior dominant directionality within voxels on the border between the thalamus and the rostral mesencephalon. Therefore, a seeding ROI was manually defined at this position (see Fig. 1e and supplementary Fig. 5b). No inclusion or exclusion ROIs were needed.

Cingulum

As the initial tractography (see panel B on Fig. 7) was not able to display subgenual and temporal parts of the cingulum, we chose to subdivide the cingulum into three respective sections as has previously been done in human studies (Jones et al. 2013; Pascalau et al. 2018). The three subsections were an "anterior cingulum" near the genu of the corpus callosum, a "dorsal cingulum" dorsal to the body of the corpus callosum, and a "temporal cingulum" located caudal to the splenium. These three subdivisions were made as individual tractographies, later to be combined on a single image. First, in the anterior subdivision, the seeding ROI was placed just anterior to the genu of the corpus callosum (see supplementary Fig. 6b), with an inclusion ROI waypoint also placed inferior to this structure (supplementary Fig. 6c) and an exclusion ROI placed at the fimbria–fornix

region (supplementary Fig. 6d), as a few single streamlines propagated into this structure in some animals. Second, a seeding ROI was placed in the white matter of the cingulate gyrus, approximately midway along its course (see Fig. 1f), to track the dorsal part of the cingulum using two nearby inclusion ROI "waypoints" selected anteriorly and posteriorly to this point, respectively, to direct the bidirectional streamline propagation along the cingulum and not across it, e.g., in a superior direction from the seeding point. Third, a seeding ROI was placed just infero–posterior to the posterior part of the lateral ventricles (supplementary Fig. 6e), between these and the mesencephalon, where ODF glyphs indicated a dominant infero-temporal direction of underlying fibers pointing towards the temporal lobe, and where a slight overlap existed between the seeding ROI and streamlines from the dorsal cingulum tractography. An inclusion ROI waypoint closer to the temporal lobe was chosen (supplementary Fig. 6f) along with an exclusion ROI positioned approximately midsagittally in the splenium of the corpus callosum, including the adjacent and inferiorly located fornix (supplementary Fig. 6g) as a few streamlines off course propagated here.

3D visualization

Using the screen capture tool in MRtrix 3 Software (Tournier et al. 2004, 2007), 180 images were taken every two degrees in a 360° rotation to complete a full rotation. This was done in both volume-rendering view as well as images of isolated individual tractographies. The respective images were then merged to a stop-motion video in iMovie (Apple Inc., US). Tractographies were merged in the same manner and overlayed with a transparency, so that both brain and tractographies had the exact same orientation and could both be appreciated in the series of images.

Results

In all limbic tractographies, a high number of streamlines were able to meet the exclusion/inclusion selection criteria and, hence, were part of the investigated tracts. The selected number of streamlines across tractographies, however, varied with the large and well-defined fiber bundles yielding higher streamline selection (see Table 2). Video material can be assessed in the electronic supplementary material. In the following, the individual tractographies are described while displaying data from one animal. See supplementary Figs. 1–6 for data from the remaining animals.

Fornix

From its origin in the hippocampus, the fimbria of the fornix (Fim) was seen to converge to form the body of the fornix (bF) just inferior to the corpus callosum. From here, the streamlines were seen to continue anteriorly in a position superior and medial to the lateral ventricle and then descend to form the column of the fornix (colF), which separates into the precommissural (PreC) and postcommissural (PostC) bundle, respectively. The precommissural bundle was then diverged inferiorly and laterally as horizontal fibers (HZ) in the basal forebrain. The postcommissural fibers were seen to continue in a posterior direction through the hypothalamus to terminate in the mammillary body, see Fig. 2. Note also the psalterium dorsale (PsD) posterior to the fimbria–fornix region. The above finding was similar across animals and bilateral.

The mammillothalamic tract (bundle of Vicq d'Azyr)

The mammillothalamic tract (MT) connects the mammillary body and the anterior part of the thalamus by curving

Table 2 Table displaying the number of selected streamlines of the 10,000 streamlines generated in each of the tractographies

Structure	JBG3 selected		JBG4 selected		JBG5 selected	
Hemisphere (right/left)	*R*	*L*	*R*	*L*	*R*	*L*
Fornix	8618	7967	8939	7325	7437	6609
Mammillothalamic tr	9041	9274	9389	9489	4106†	4151†
Stria terminalis	9241	8576	8921	9165	9033	8930
Stria medullaris	6918	4465	8802	5167	7640	6997
Habenulo–interpeduncular tr	9743	9675	9361	9832	9609	9772
Anterior cingulum	1716	1710	611	273	968	1410
Dorsal cingulum	1499	1536	1950	2008	1482	834
Temporal cingulum	1247	849	855	724	617	699

Since the generated number of streamlines was the same in all performed tractographies, the displayed numbers above correspond to arbitrary probability measures of the investigated tracts, although this can normally be evaluated by the ratio of generated and selected streamlines. All ratios were above the noise floor of streamlines to visualize the tract of interest. (†) Note this animal had an inclusion ROI, which reduced the number of selected streamlines

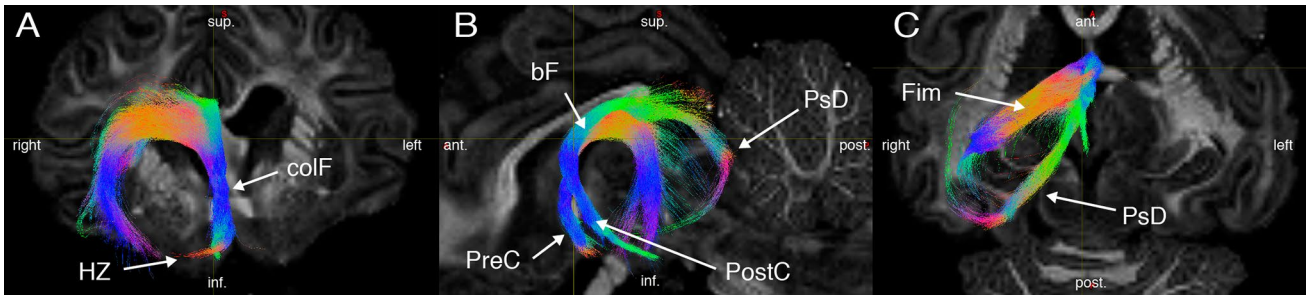

Fig. 2 Orthogonal view displaying the right fornix of JBG5, not cropped to slab for overview. **a** Coronal, **b** sagittal, **c** axial view, respectively. Note the column of the fornix (colF) and the small red horizontal fibers (HZ) of the precommissural fibers (PreC) seen in image **a**, which together with the postcommissural fibers (PostC) and the body of the fornix (bF) can be seen in **b**. The fimbria–fornix (Fim) are seen in **a**–**c**. Psalterium dorsale (PsD) is seen in **b**, **c**. Red, right/left; Blue, superior/inferior; Green, anterior/posterior

anterior to the latter. In the coronal plane, the well-defined tract is seen as a circular fiber bundle, which together with the contralateral tract and the two postcommissural fornix bundles constitute four characteristic dots, which are also easily identified macroscopically on histological sections (Figs. 1b and 3). The tract showed close consistency bilaterally in all animals.

Stria terminalis

The stria terminalis (ST) is a well-defined and prominent fiber bundle connecting the amygdala to the basal forebrain and the hypothalamus. The tractography data display a course originating at the border of the amygdala, from where the fiber bundle is seen to ascend close to the centrum semiovale and lateral ventricles. It then takes a curved turn of approximately 160–180° to descend in a medial direction, running lateral and anterior to the thalamus. The streamlines are then seen to proceed either anteriorly or posteriorly in relation to the anterior commissure. The largest, posterior group terminates either in the bed nucleus of the ST (BNst) or in the hypothalamus. The smaller anterior group can be found near the nucleus accumbens (NAcc) and the basal forebrain, where the majority of them terminate with some streamlines, however, continuing further anterior in the ventral internal capsule. A small group of streamlines is also deviating from the main fiber bundle at the centrum semiovale. See Fig. 4. The contralateral ST and the ST of the other animals displayed a similar consistent distribution.

Stria medullaris

Streamlines displaying the stria medullaris (SM) formed a distinct bundle near the midline in the center of the brain. They connected the habenula and the septal region immediately superior and posterior to the anterior commissure and near the bed nucleus of the stria terminalis. Here, streamlines were situated between the fornix column (medially

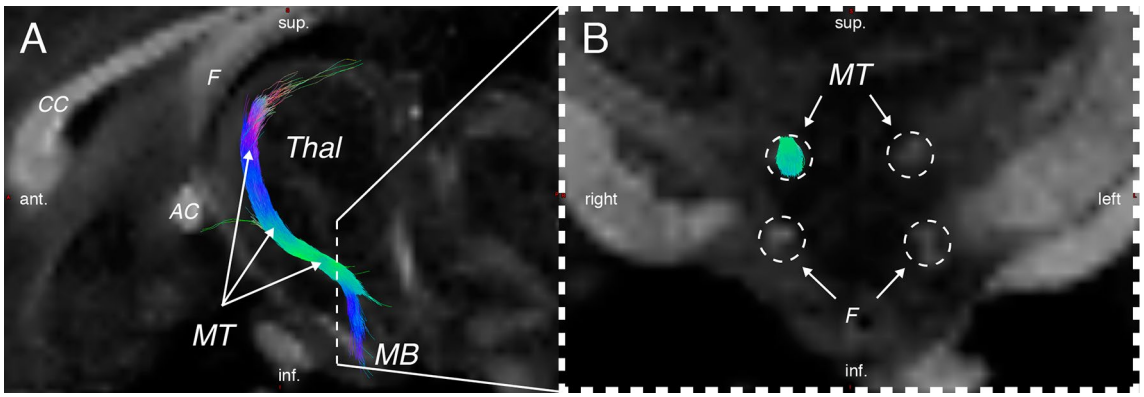

Fig. 3 Tractography of the right mammillothalamic tract (MT) of JBG4. Image **a** is a sagittal view displaying the course of the tract from the mammillary body (MB) (bottom) to the anterior thalamus (Thal) (top), not cropped to slab. Image **b** is an enlarged cross-sectional (coronal) view of the initial part of the tract (dashed plane in image **a**), cropped to slab, where the tract is in near proximity to the postcommissural fornix (F) (dashed circles), which also display high anisotropy. *CC* corpus callosum, *AC* anterior commissure. Red, right/left. Blue, superior/inferior. Green, anterior/posterior

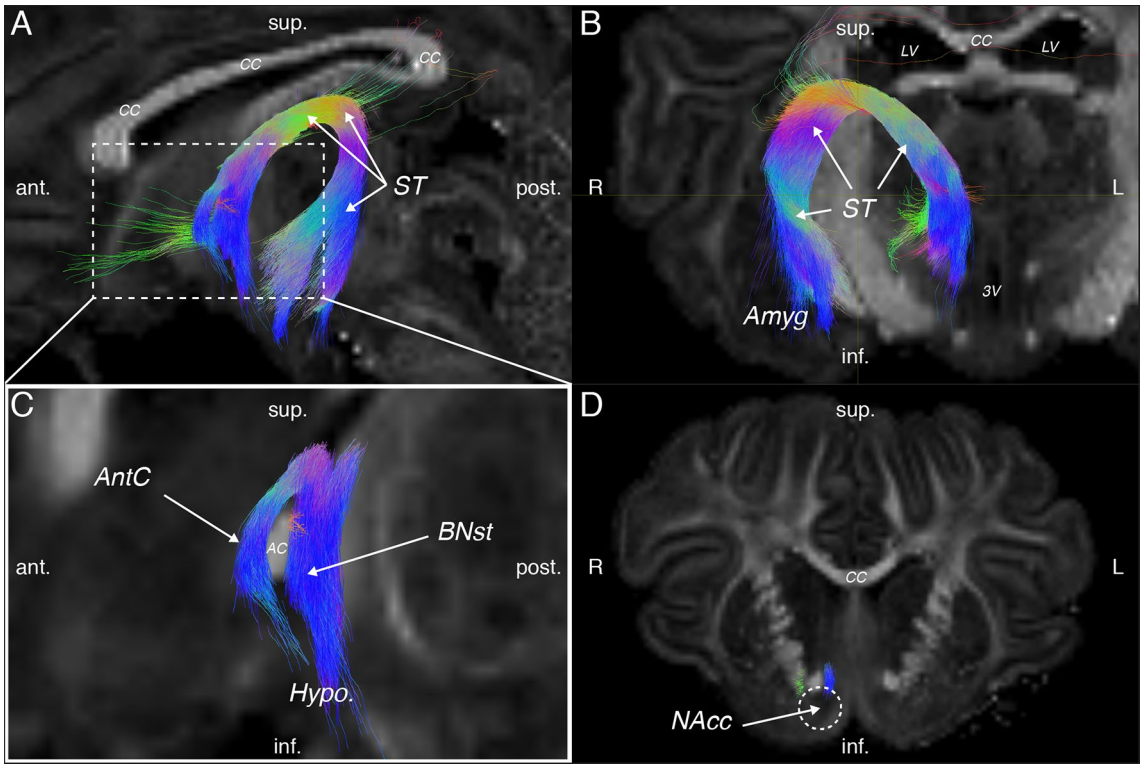

Fig. 4 Tractography of the right stria terminalis (ST) of JBG3. **a**, **b** Are not cropped to slab for overview, **c**, **d** are cropped to slab. Image **a** is a sagittal view providing an overview of the ST. Image **b** is coronal view where the lateral–medial direction of the ST can be appreciated. The fiber bundle is seen to originate in the amygdala (Amyg). Image **c** is a closer sagittal view, where streamlines divide and pass either posterior or anterior (AntC) to the anterior commissure (AC). The posterior fibers terminate in the areas close to the bed nucleus of the stria terminalis (BNst), anterior commissure, and hypothalamus (Hypo). Image **d** displays the anterior fibers terminating near the nucleus accumbens (NAcc). *3V* third ventricle, *CC* corpus callosum. Red, right/left. Blue, superior/inferior. Green, anterior/posterior

positioned) and the stria terminalis (laterally positioned) before they continued further inferior adjacent to the postcommissural fornix to terminate near the lateral preoptic area of the hypothalamus. On their way, streamlines curved anterior and superior to the thalamus. The course was similar to the mammillothalamic tract (MT), but was both more anteriorly and superiorly located and forming a larger curvature. See Fig. 5. The data were consistent bilaterally and across animals.

The habenulo-interpeduncular tract (fasciculus retroflexus)

From its top at the habenula, the habenulo-interpeduncular tract (fRF) was found to descend on the posterior side of the thalamus, where the tract was positioned between the thalamus and the mesencephalon. In the ventro-medial part of the mesencephalon, it reached the interpeduncular nucleus. The majority of streamlines, however, turned in a posterior direction to terminate near the midline of the dorsal brain stem at the level of the lower mesencephalon and upper pons. Some streamlines were also found to terminate

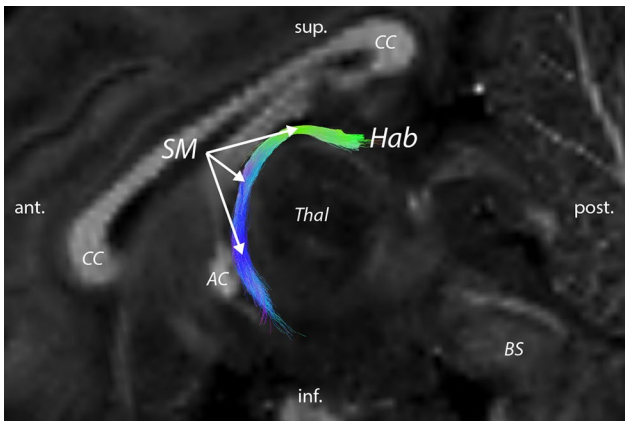

Fig. 5 A sagittal view of the left stria medullaris (SM) tractography of JBG4. The fiber bundle is seen to connect the habenula (Hab) with septal areas near the anterior commissure (AC) curving anterior to the thalamus (Thal). *CC* corpus callosum, *BS* brain stem. Red, right/left. Blue, superior/inferior. Green, anterior/posterior

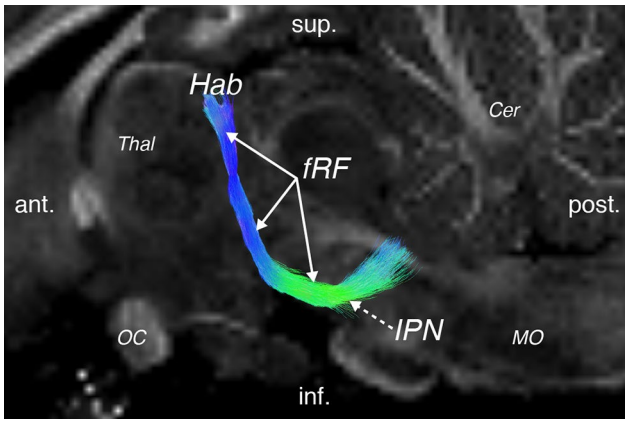

Fig. 6 Sagittal view of the tractography of the left habenulo-interpeduncular tract, also known as the fasciculus retroflexus (fRF), of JBG5 not cropped to slab. The course from the habenula (Hab) to the interpeduncular nucleus (IPN, dashed arrow) in the mesencephalon can be appreciated. Note the streamlines continuing from the interpeduncular nucleus to the dorsal brainstem. *Thal* thalamus, *OC* optic chiasm, *Cer* cerebellum, *MO* medulla oblongata. Red, right/left. Blue, superior/inferior. Green, anterior/posterior

in the interpeduncular nucleus. See Fig. 6. Very similar results were found in the contralateral hemisphere and in the other animals. The most varying, but still discrete, difference between animals were the distance the streamlines propagated into the habenular complex.

Cingulum

The cingulum generally had a higher ratio of generated streamlines versus selected streamlines than the other tracts investigated and hence lower probability; see Table 2 and later discussion. The "anterior cingulum" is curving around the genu of the corpus callosum from the subgenual Brodmann area 25 (BA25) and nearby septal areas. From the genu of the corpus callosum, the "dorsal cingulum" is seen to generally follow the cingulate gyrus, and it is located just superior to the corpus callosum on each medial hemisphere. It is positioned slightly more lateral to the most dorsal streamlines of the anterior cingulum subdivision. Note the streamlines propagating towards the frontal pole and dorsal prefrontal cortex. On the posterior part, most streamlines of the "dorsal cingulum" subdivision terminate close to the posterior centrum semiovale area, from where the streamlines of the "temporal cingulum" subdivision continue inferiorly and laterally around the posterior part of the lateral ventricles to enter the temporal lobe, predominantly near parahippocampal areas as the presubiculum, the subiculum, the ento- and the perirhinal cortices. See Fig. 7. The results were similar on the contralateral hemisphere and across animals.

Discussion

Several limbic system pathways in the minipig were distinctly visualized by the use of ex vivo tractography. This has not previously been done and the limbic system pathways are currently not well described in this animal. Although difficulties have been described in visualizing smaller limbic connections in human studies (Concha et al. 2005), it was, however, possible to visualize such connections, e.g., the mammillothalamic tract in the minipig using an ex vivo setup. We, hence, provide a new neuroanatomical insight which we evaluate against the known anatomy from other species and human data below.

Fornix

The distribution of the fornix had similarities with a human anatomy (Pascalau et al. 2018) including the precommissural horizontal fibers described by Kamali et al. (2015). Tracing studies in macaques have also found hippocampal–thalamic connections via the fornix (Aggleton et al. 1986). The termination of streamlines in the hypothalamus and its mammillary bodies were in gray matter. However, the diffuse delineation of the hypothalamus presents a challenge when evaluating correct streamline termination in gray matter contrary to the false-positive streamlines continuing around gray matter structures as has previously been described (Dyrby et al. 2007). Similarly, the fading of the streamlines representing the psalterium dorsale may represent false positives as no clear termination point is seen, and as the psalterium is known to be a largely commissural structure (Brodal 1969). Due to the midsagittal exclusion ROI, the commissural fibers are not present in the data and, hence, only uncrossed fibers may be seen. As have previously been described by Concha et al. (2005), we, likewise, encountered partial volume effects lowering the anisotropy within the juxtaventricular voxels. Due to the anatomical position of the fornix and hippocampus, this may very well have caused streamlines connecting these structures to terminate prematurely at the border of the hippocampus, since the cut-off adjusted to avoid false positives in this case would terminate such streamlines. The unilateral approach of tractography did not display the commissural fornix fibers, and since an overlap between the respective fornices at the fornix body or column was inevitable, this was a compromise made.

The mammillothalamic tract

As an original part of the Papez circuit, the mammillothalamic tract was, also in the minipig, seen to connect the mammillary bodies to the anterior thalamus, hence finishing

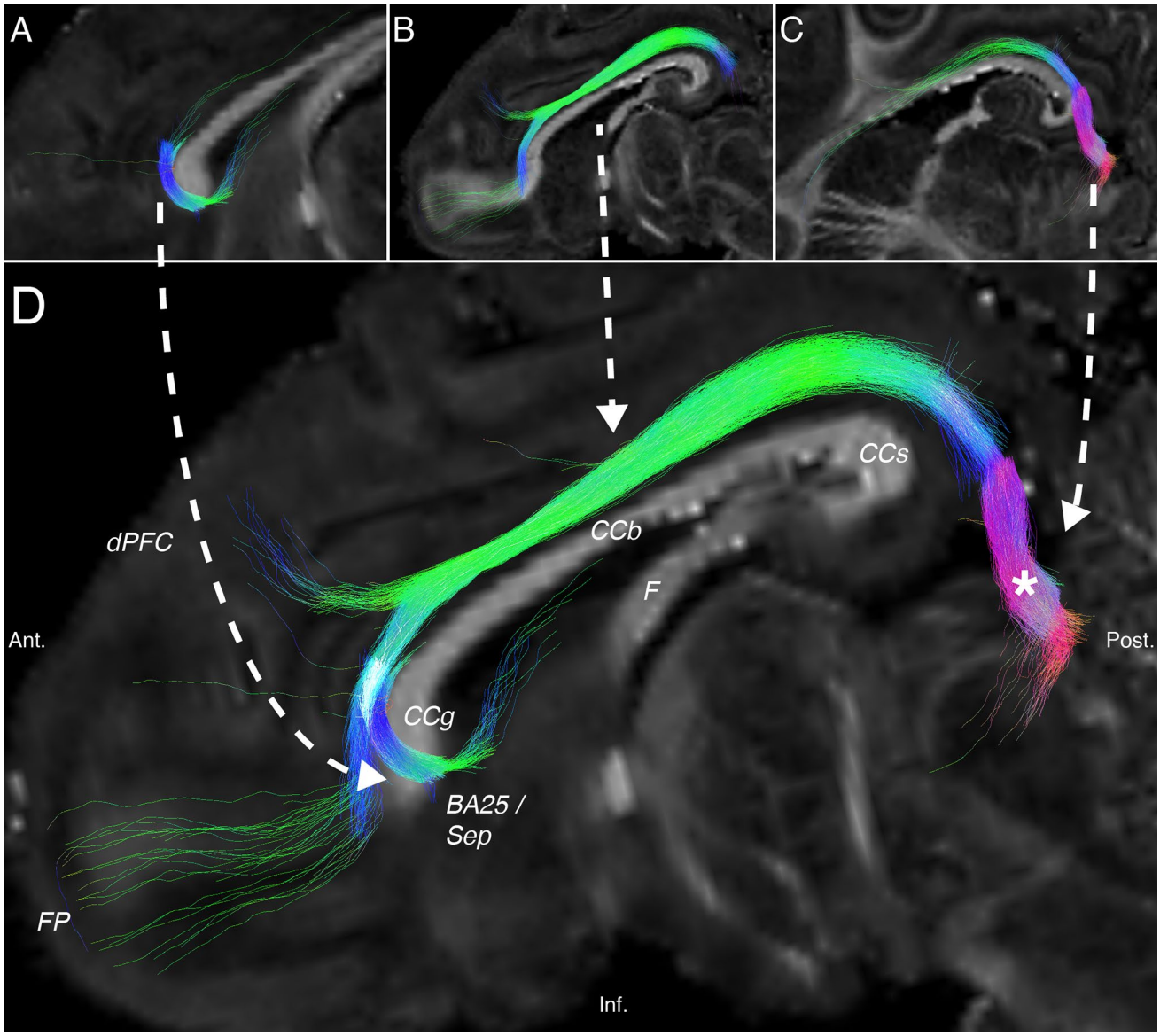

Fig. 7 Tractographies of the right cingulum of JBG3 not cropped to slab for overview. All images are in sagittal view. Panel **a** displays the "anterior cingulum" subdivision curving around the genu of the corpus callosum (CCg) to areas near the septum (Sep) and Brodmann area 25 (BA25). Panel **b** displays the "dorsal cingulum" above the body of the corpus callosum (CCb) with the fornix (F) further inferior across the lateral ventricle. The "dorsal cingulum" curves around the splenium of the corpus callosum (CCs) near the posterior lateral ventricle, from where the "temporal cingulum" is also seen in panel **c**, where a purple–red color shift can be appreciated as streamlines turn and head towards the parahippocampal areas in the temporal lobe (asterisk). Panel **d** displays the combined three subdivisions merged on one image. The temporal and dorsal subdivision is closely overlapping while a small medial/lateral gap is found between the anterior and dorsal subdivision near the genu of the corpus callosum. *dPFC* dorsal prefrontal cortex, *FP* frontal pole. Red, right/left. Blue, superior/inferior. Green, anterior/posterior

the pathway from the hippocampus to the thalamus (Papez 1937; Aggleton and Brown 1999). The tract was well defined in all investigated animals and had a rather direct course comparable with human studies (Kwon et al. 2010), although the respective interspecies location of the connected structures changed the course slightly. A recent translational MT lesion study has investigated its role in temporal memory in rats (Nelson and Vann 2017), but, currently, no studies have been carried out in minipigs. The knowledge of the MT in the minipig may, hence, facilitate similar studies in a large animal model.

Stria terminalis

De Olmos and Ingram (1972) have previously performed a highly detailed silver impregnation study of the rat

stria terminalis to study the projections of this pathway. These were described in segregated groups with subdivisions, and our data were generally consistent with their findings, although such a histological division of components was not possible using tractography. Especially, this was true for the described "dorsal component" of the ST, which consists of a supracommissural division, further subdivided in a parolfactory radiation and a hypothalamic radiation, and a retrocommissural division (De Olmos and Ingram 1972). The supracommissural parolfactory radiation was described to project to areas including the bed nucleus of the stria terminalis, septum, and the accumbens nucleus, among others, where the streamlines in our study were also found. The hypothalamic radiation was described to project to the medial suprachiasmatic region of the hypothalamus, which could similarly be seen in our data; only with a small number of streamlines and not projecting as far into the hypothalamus. Moreover, it could not be evaluated which certain previously described hypothalamic nuclei the streamlines projected to, since these areas display low anisotropy hindering streamline propagation. As for the retrocommissural division of the "dorsal component", our data were also comparable with the histological findings of De Olmos and Ingram (1972) with streamlines found in the hypothalamic area. Their "ventral component" was described to project near the more basally located white matter tracts, e.g., the medial forebrain bundle, to the bed nucleus of the stria terminalis, hypothalamus, and premammillary areas, but it was not evident in our data, which is due to the dorsal seeding strategy. Our tractography data, hence, found streamlines in the "dorsal component", but generally did not provide the detailed segregation obtained through selective amygdala lesions and subsequent axonal visualization. Likewise, commissural projections could not be investigated due to the unilateral tractography as discussed previously in the case of the fornix. Other tractography studies have previously investigated the ST in humans and revealed a very similar ST anatomical distribution (Kamali et al. 2015, 2016), however, with fewer details probably due to the human in vivo setup and limited spatial resolution. In our data, two minor groups of streamlines were seen fading from the centrum semiovale and anteriorly in the ventral internal capsule, respectively. These groups are likely to represent false positives, since they have no clear termination point in gray matter. As is the case with the fornix, the septal, and hypothalamic regions are difficult streamline termination points to evaluate due to their location and diffuse delineation. This issue of false positives represents a challenge in tractography, since evaluation of the false-positive streamlines ultimately relies on preexisting knowledge or subsequent verification with neuronal tracing.

Stria medullaris

The SM has previously been described to form an associational connection from the habenula to the septal nuclei, the basal forebrain, hypothalamus, and mesencephalon (Antolin-Fontes et al. 2015; Herkenham and Nauta 1977). The general course of the SM was found to be similar in our data; however, the connections to these complex areas are difficult termination points to evaluate as was the case for the fornix and the stria terminalis. Interestingly, in rats, some fibers from the habenula have previously been traced to supra- and postcommissural septal areas and also areas in proximity to the postcommissural fornix (Herkenham and Nauta 1977), where the streamlines in the tractography data were also found. The connections to mesencephalic areas including the ventral tegmental area were not seen in our data, which may be due to the long course of such fibers, which, furthermore, traversed complex nucleated areas in the basal tel- and diencephalon. Streamlines were not found in septal nuclei in front of the anterior commissure. Connections to the globus pallidus have also been suggested to constitute a linkage between the basal ganglia and limbic system (Hikosaka et al. 2008). This was, however, not evident from our studies and may very well be due to difficulties in tracking such a minor group of fibers traversing the massive projecting fiber connections constituting the internal capsule.

The habenulo-interpeduncular tract (fasciculus retroflexus)

This bundle of habenula efferent to the interpeduncular nucleus was, like the stria medullaris, very well defined and in accordance with the previous tracing studies in rats (Woolf 1991). Interestingly, the streamlines not only did terminate in the nucleus itself, but many also continued to the dorsal part of the mesencephalon and upper pons. This is in accordance with previously described efferent connections from the interpeduncular nucleus to the median and dorsal raphe nuclei as well as the dorsal and laterodorsal tegmental regions in murine studies (Antolin-Fontes et al. 2015; Groenewegen et al. 1986; Lima et al. 2017). The streamlines terminated shortly after entering the nucleated area of the habenular complex lowering the anisotropy within the voxels. This was similar to the case of the stria terminalis. The distance the streamlines propagated before terminating displayed a small variation, which may be caused by subtle differences in voxel–FA values within the respective habenular complexes.

Cingulum

A previous study has argued for a misleading representation of the cingulum by handling it as a single anatomical

unit (Jones et al. 2013), as earlier neuronal tracing studies in the rhesus monkey display a very complex connectivity of the cingulum and projecting areas (Mufson and Pandya 1984). Jones et al. considered the possibility that the many short associating fibers within the cingulum gives an appearance of a united tract, although this may not be the case. Based on these neuronal tracing studies, Jones et al., therefore, suggested segregating the cingulum tractographically into three groups called "the parahippocampal", "retrosplenial", and "subgenual" subdivision, respectively (Jones et al. 2013). Initially, we only made the tractography of the dorsal subdivision of the cingulum [corresponding to the "retrosplenial" subdivision (Jones et al. 2013)]. Although we used waypoints, we chose this initial approach as it was similar to what was used by previous tractography studies of the cingulum (Thiebaut de Schotten et al. 2012). It is evident from our data that in the minipig, this fails to display subgenual and temporal streamlines, which at least in humans is known to be a feature of the cingulum (Jones et al. 2013; Thiebaut de Schotten et al. 2012; Pascalau et al. 2018). A contributing factor to this may very well be the complex white matter areas that the cingulum traverses, especially in the subgenual and centrum semiovale regions. Furthermore, it seems that the white matter containing the temporal cingulum streamlines is very narrow making it susceptible to partial volume effects, which was especially evident in JBG5 (see also supplementary Fig. 6e). Using the three-subdivision strategy, we were able to display streamlines to the subgenual and parahippocampal regions. Nevertheless, the data failed to display the smaller association fibers, e.g., within the cingulate gyrus, and also fibers to the parietal lobe as has been seen in other species (Thiebaut de Schotten et al. 2012; Catani et al. 2013; Mufson and Pandya 1984; Pascalau et al. 2018). These shortcomings may have to do with the preferred directionality within individual voxels continuing along the cingulum rather than leaving it. Furthermore, the cingulate gyrus is very small in the minipig, so the distance from the center of the cingulum to the cortex is minimal, which may disguise streamlines actually terminating at the border of the cingulum before being readily recognizable from the other continuing streamlines. The apparent "division" of streamlines at the genu of the corpus callosum toward either the BA25 and septal region or more frontal areas is similar to what has been found in monkeys (Thiebaut de Schotten et al. 2012). The rather sudden termination of streamlines from the anterior subdivision dorsal to the genu of the corpus callosum may also have to do with the relatively small cingulate gyrus of the minipig, which is, hence, susceptible to partial volume effects. As for the evaluation of correct termination of streamlines, i.e., evaluation of false positives, the cingulum tractography is facing the same obstacles as some of the other limbic structures described above, which can be seen in the minor group of streamlines propagating towards the dPFC or frontal pole.

General comments and method considerations

Recently, a study of the human limbic pathways has been made, where tractography was compared with macro-anatomical fiber dissections (Pascalau et al. 2018). Our study, thus, provides a porcine analogue supported by micro-anatomical knowledge from an established histology atlas, and where the use of high-quality ex vivo DWI yielded a detailed tractography. This overcame previously described difficulties with tractography of limbic structures related to resolution issues (Concha et al. 2005). There are yet inherent challenges in tractography besides resolution issues, e.g., false-positive evaluation. In agreement with a recent and comprehensive methodological study (Maier-Hein et al. 2017) describing such challenges, we propose that a detailed prior anatomical knowledge is important to integrate in tractography, especially when addressing issues as false positives. This problem was still evident in our study perhaps due to the complexity of the regions connected by limbic pathways. These regions are both difficult to precisely delineate and generally have, at least in other species, numerous connecting pathways. Even though a previous histological knowledge from a detailed atlas is useful, it cannot fully assess false-positive streamlines as can be done by the use of neuronal tracing, which is a methodological shortcoming affecting the specificity of the results. Moreover, the cut-off for streamline termination was found to have a marked effect on the streamline distribution and number of suspected false positives, which could probably be ascribed to the complex white matter areas or low anisotropic gray matter regions traversed by the investigated limbic pathways. We chose a relatively high cut-off value to address this problem, which yielded fewer false positives skirting around nucleated gray matter areas, but, on the other hand, terminated streamlines immediately after entering the gray matter or complex white matter areas. This issue was also described previously (Dyrby et al. 2007). It is likely that minor connections from limbic structures may, therefore, not be presented in the tractography data, e.g., in the above-mentioned case of the cingulum, which introduces false negatives in the data. This issue may, furthermore, have been compounded by partial volume effects, e.g., in the juxtaventricular voxels where the otherwise highly anisotropic white matter suffers from the low anisotropy within the adjacent ventricles. As some of the investigated limbic pathways traverse small regions containing only a few voxels, e.g., the cingulum in the cingulate gyrus, it is plausible that such partial volume effects will affect the data seen in the variability of streamlines in Table 2. In the case of the

amygdala with its large gray matter area, it was not possible to display in which subdivisions the stria terminalis originated, although the amygdala is known to have several nuclei with different inputs and outputs (Swanson and Petrovich 1998; Janak and Tye 2015; Murray 2007). This issue is well known in tractography, which cannot reliably visualize connections that traverse gray matter or low anisotropical areas (Donahue et al. 2016; Dyrby et al. 2007). Such investigations are currently limited to neuronal tracing studies, which are also needed for final verification of neuronal connections, although for obvious reasons not applicable in human studies (Bech et al. 2018). Previously, Jelsing et al. performed a tracing study of the Göttingen minipig prefrontal cortex (Jelsing et al. 2006) combining biotinylated dextran amine (BDA)-neuronal tracing with in vivo manganese-MRI tracing. While manganese was found to be a sensitive tracer with good correlation to BDA tracing, the current tractography methodology enables an easier and faster alternative able to display even smaller pathways reliably and in detail as was done in our study. When compared to histological methods in general, tractography also avoids artefacts secondary to serial slicing of brain tissue and permits an easy 3D representation of white matter connections at the expense of a lower spatial resolution. Despite being based on advanced mathematical models rather than physical tracer transportation, tractography yet proves a valuable and sophisticated method excellent for hypothesis generation when considering method limitations, e.g., in the sense of false positives and gray matter areas.

Conclusion

Although it has previously been difficult to perform tractography of some limbic structures, the use of high-quality ex vivo tractography seemed to overcome such challenges. This yielded a new visualization and three-dimensional anatomical overview for understanding the major connections within the limbic system of the Göttingen minipig.

Our results are generally closely related to results found in other species, including humans, in both tractography and neuronal tracing studies. Inherent methodological challenges of tractography were evident in our data, especially in the sense of false-positive streamlines. Moreover, some of the previously described minor connections found in neuronal tracing and silver impregnation studies in other species were not visible in our data. It is not known whether this is due to interspecies differences or due to failure of the method to display such connections, but the latter is proposed. This underlines the importance of preexisting neuroanatomical knowledge when using and evaluating tractography. Conversely, this method permits the investigation of numerous white matter tracts in a single brain within a reasonable time frame, thereby making it extremely suitable for hypothesis generation.

Our proposed seeding strategies used in this study provide a useful way to reproduce tractography of limbic structures, since our results displayed a high consistency throughout all investigated animals. Similar to what has previously been done in human studies (McIntosh et al. 2008), quantifiable altered white matter connectivity may be used in future studies to measure pathological progression, which can facilitate novel translational models involving the investigated limbic structures. Furthermore, since we succeeded in visualizing several limbic pathways consistently, our results points to the possibility of using tractography-guided implementation of deep-brain stimulation electrodes similar to previous studies (Coenen et al. 2011; Petersen et al. 2017). With the increased neuroanatomical knowledge of the Göttingen minipig limbic system, we have paved the way for future studies. Moreover, the close resemblance of our results with such found, e.g., in monkeys and humans, suggests that the minipig may very well be an excellent translational animal model for studying a variety of limbic system-related diseases.

Acknowledgements We would like to acknowledge the previously given funding from the Novo Nordisk Foundation (Grant no. NNF15OC00015680), the Jascha Foundation (Grant no. 5559), "Fonden for Neurologisk Forskning", and "Simon Fougner Hartmanns Familiefond" to permit us to carry out this study.

Compliance with ethical standards

Conflict of interest The authors declare that they have no conflict of interest.

Ethical approval All applicable international, national, and/or institutional guidelines for the care and use of animals were followed. All procedures performed in studies involving animals were approved by and in accordance with the ethical standards of the Danish National Council of Animal Research Ethics (protocol number 2015-15-0201-00965).

References

Aggleton JP, Brown MW (1999) Episodic memory, amnesia, and the hippocampal-anterior thalamic axis. Behav Brain Sci 22(3):425–444

Aggleton JP, Desimone R, Mishkin M (1986) The origin, course, and termination of the hippocampothalamic projections in the macaque. J Comp Neurol 243(3):409–421. https://doi.org/10.1002/cne.902430310

Antolin-Fontes B, Ables JL, Gorlich A, Ibanez-Tallon I (2015) The habenula–interpeduncular pathway in nicotine aversion and withdrawal. Neuropharmacology 96(Pt B):213–222. https://doi.org/10.1016/j.neuropharm.2014.11.019

Basser PJ, Mattiello J, LeBihan D (1994) MR diffusion tensor spectroscopy and imaging. Biophys J 66(1):259–267. https://doi.org/10.1016/s0006-3495(94)80775-1

Bech J, Glud AN, Sangill R, Petersen M, Frandsen J, Orlowski D, West MJ, Pedersen M, Sorensen JCH, Dyrby TB, Bjarkam CR

(2018) The porcine corticospinal decussation: a combined neuronal tracing and tractography study. Brain Res Bull 142:253–262. https://doi.org/10.1016/j.brainresbull.2018.08.004

Behrens TE, Berg HJ, Jbabdi S, Rushworth MF, Woolrich MW (2007) Probabilistic diffusion tractography with multiple fibre orientations: What can we gain? NeuroImage 34(1):144–155. https://doi.org/10.1016/j.neuroimage.2006.09.018

Bjarkam CR, Cancian G, Glud AN, Ettrup KS, Jorgensen RL, Sorensen JC (2009) MRI-guided stereotaxic targeting in pigs based on a stereotaxic localizer box fitted with an isocentric frame and use of SurgiPlan computer-planning software. J Neurosci Methods 183(2):119–126. https://doi.org/10.1016/j.jneumeth.2009.06.019

Bjarkam CR, Glud AN, Orlowski D, Sorensen JC, Palomero-Gallagher N (2017a) The telencephalon of the Gottingen minipig, cytoarchitecture and cortical surface anatomy. Brain Struct Funct. https://doi.org/10.1007/s00429-016-1327-5

Bjarkam CR, Nielsen MS, Glud AN, Rosendal F, Mogensen P, Bender D, Doudet D, Moller A, Sorensen JC (2008) Neuromodulation in a minipig MPTP model of Parkinson disease. Br J Neurosurg 22(Suppl 1):S9–12. https://doi.org/10.1080/02688690802448285

Bjarkam CR, Orlowski D, Tvilling L, Bech J, Glud AN, Sorensen JH (2017b) Exposure of the pig CNS for histological analysis: a manual for decapitation, skull opening, and brain removal. J Vis Exp JoVE 122:45–48. https://doi.org/10.3791/55511

Broca P (1877) Sur la circonvolution limbique et la scissure limbique. Bulletins et Mémoires de la Société d'Anthropologie de Paris 646–657

Brodal A (1969) Neurological anatomy, 2nd edn. Oxford University Press, Oxford

Catani M, Dell'acqua F, Thiebaut de Schotten M (2013) A revised limbic system model for memory, emotion and behaviour. Neurosci Biobehav Rev 37(8):1724–1737. https://doi.org/10.1016/j.neubiorev.2013.07.001

Christensen AB, Sorensen JCH, Ettrup KS, Orlowski D, Bjarkam CR (2018) Pirouetting pigs: a large non-primate animal model based on unilateral 6-hydroxydopamine lesioning of the nigrostriatal pathway. Brain Res Bull 139:167–173. https://doi.org/10.1016/j.brainresbull.2018.02.010

Coenen VA, Allert N, Madler B (2011) A role of diffusion tensor imaging fiber tracking in deep-brain stimulation surgery: DBS of the dentato–rubro–thalamic tract (drt) for the treatment of therapy-refractory tremor. Acta Neurochir 153(8):1579–1585. https://doi.org/10.1007/s00701-011-1036-z

Concha L, Gross DW, Beaulieu C (2005) Diffusion tensor tractography of the limbic system. AJNR Am J Neuroradiol 26(9):2267–2274

De Olmos JS, Ingram WR (1972) The projection field of the stria terminalis in the rat brain. An experimental study. J Comp Neurol 146(3):303–334. https://doi.org/10.1002/cne.901460303

Dolezalova D, Hruska-Plochan M, Bjarkam CR, Sorensen JC, Cunningham M, Weingarten D, Ciacci JD, Juhas S, Juhasova J, Motlik J, Hefferan MP, Hazel T, Johe K, Carromeu C, Muotri A, Bui J, Strnadel J, Marsala M (2014) Pig models of neurodegenerative disorders: Utilization in cell replacement-based preclinical safety and efficacy studies. J Comp Neurol 522(12):2784–2801. https://doi.org/10.1002/cne.23575

Donahue CJ, Sotiropoulos SN, Jbabdi S, Hernandez-Fernandez M, Behrens TE, Dyrby TB, Coalson T, Kennedy H, Knoblauch K, Van Essen DC, Glasser MF (2016) Using diffusion tractography to predict cortical connection strength and distance: a quantitative comparison with tracers in the monkey. J Neurosci 36(25):6758–6770. https://doi.org/10.1523/jneurosci.0493-16.2016

Dyrby TB, Baare WF, Alexander DC, Jelsing J, Garde E, Sogaard LV (2011) An ex vivo imaging pipeline for producing high-quality and high-resolution diffusion-weighted imaging datasets. Hum Brain Mapp 32(4):544–563. https://doi.org/10.1002/hbm.21043

Dyrby TB, Innocenti GM, Bech M, Lundell H (2018) Validation strategies for the interpretation of microstructure imaging using diffusion MRI. NeuroImage 182:62–79. https://doi.org/10.1016/j.neuroimage.2018.06.049

Dyrby TB, Sogaard LV, Parker GJ, Alexander DC, Lind NM, Baare WF, Hay-Schmidt A, Eriksen N, Pakkenberg B, Paulson OB, Jelsing J (2007) Validation of in vitro probabilistic tractography. NeuroImage 37(4):1267–1277. https://doi.org/10.1016/j.neuroimage.2007.06.022

Ettrup KS, Glud AN, Orlowski D, Fitting LM, Meier K, Soerensen JC, Bjarkam CR, Alstrup AK (2011) Basic surgical techniques in the Gottingen minipig: intubation, bladder catheterization, femoral vessel catheterization, and transcardial perfusion. J Vis Exp JoVE 52(52):2652. https://doi.org/10.3791/2652

Ettrup KS, Sorensen JC, Bjarkam CR (2010) The anatomy of the Gottingen minipig hypothalamus. J Chem Neuroanat 39(3):151–165. https://doi.org/10.1016/j.jchemneu.2009.12.004

Fang X, Mou Y, Huang Z, Li Y, Han L, Zhang Y, Feng Y, Chen Y, Jiang X, Zhao W, Sun X, Xiong Z, Yang L, Liu H, Fan D, Mao L, Ren L, Liu C, Wang J, Li K, Wang G, Yang S, Lai L, Zhang G, Li Y, Wang J, Bolund L, Yang H, Wang J, Feng S, Li S, Du Y (2012) The sequence and analysis of a Chinese pig genome. GigaScience 1(1):16. https://doi.org/10.1186/2047-217x-1-16

Glud AN, Hedegaard C, Nielsen MS, Sorensen JC, Bendixen C, Jensen PH, Larsen K, Bjarkam CR (2010) Direct gene transfer in the Gottingen minipig CNS using stereotaxic lentiviral microinjections. Acta Neurobiol Exp 70(3):308–315

Glud AN, Hedegaard C, Nielsen MS, Sorensen JC, Bendixen C, Jensen PH, Mogensen PH, Larsen K, Bjarkam CR (2011) Direct MRI-guided stereotaxic viral mediated gene transfer of alpha-synuclein in the Gottingen minipig CNS. Acta Neurobiol Exp 71(4):508–518

Gomes N, Soares SC, Silva S, Silva CF (2018) Mind the snake: fear detection relies on low spatial frequencies. Emotion (Washington, DC) 18(6):886–895. https://doi.org/10.1037/emo0000391

Groenewegen HJ, Ahlenius S, Haber SN, Kowall NW, Nauta WJ (1986) Cytoarchitecture, fiber connections, and some histochemical aspects of the interpeduncular nucleus in the rat. J Comp Neurol 249(1):65–102. https://doi.org/10.1002/cne.902490107

Herkenham M, Nauta WJ (1977) Afferent connections of the habenular nuclei in the rat. A horseradish peroxidase study, with a note on the fiber-of-passage problem. J Comp Neurol 173(1):123–146. https://doi.org/10.1002/cne.901730107

Hikosaka O, Sesack SR, Lecourtier L, Shepard PD (2008) Habenula: crossroad between the basal ganglia and the limbic system. J Neurosci 28(46):11825–11829. https://doi.org/10.1523/jneurosci.3463-08.2008

Huff W, Lenartz D, Schormann M, Lee SH, Kuhn J, Koulousakis A, Mai J, Daumann J, Maarouf M, Klosterkotter J, Sturm V (2010) Unilateral deep brain stimulation of the nucleus accumbens in patients with treatment-resistant obsessive-compulsive disorder: outcomes after one year. Clin Neurol Neurosurg 112(2):137–143. https://doi.org/10.1016/j.clineuro.2009.11.006

Janak PH, Tye KM (2015) From circuits to behaviour in the amygdala. Nature 517(7534):284–292. https://doi.org/10.1038/nature14188

Jelsing J, Hay-Schmidt A, Dyrby T, Hemmingsen R, Uylings HB, Pakkenberg B (2006) The prefrontal cortex in the Gottingen minipig brain defined by neural projection criteria and cytoarchitecture. Brain Res Bull 70(4–6):322–336. https://doi.org/10.1016/j.brainresbull.2006.06.009

Jenkinson M, Beckmann CF, Behrens TE, Woolrich MW, Smith SM (2012) FSL NeuroImage 62(2):782–790. https://doi.org/10.1016/j.neuroimage.2011.09.015

Jones DK (2004) The effect of gradient sampling schemes on measures derived from diffusion tensor MRI: a Monte Carlo study. Magn Reson Med 51(4):807–815. https://doi.org/10.1002/mrm.20033

Jones DK, Christiansen KF, Chapman RJ, Aggleton JP (2013) Distinct subdivisions of the cingulum bundle revealed by diffusion MRI fibre tracking: implications for neuropsychological investigations. Neuropsychologia 51(1):67–78. https://doi.org/10.1016/j.neuropsychologia.2012.11.018

Kamali A, Sair HI, Blitz AM, Riascos RF, Mirbagheri S, Keser Z, Hasan KM (2016) Revealing the ventral amygdalofugal pathway of the human limbic system using high spatial resolution diffusion tensor tractography. Brain Struct Funct 221(7):3561–3569. https://doi.org/10.1007/s00429-015-1119-3

Kamali A, Yousem DM, Lin DD, Sair HI, Jasti SP, Keser Z, Riascos RF, Hasan KM (2015) Mapping the trajectory of the stria terminalis of the human limbic system using high spatial resolution diffusion tensor tractography. Neurosci Lett 608:45–50. https://doi.org/10.1016/j.neulet.2015.09.035

Kotter R, Stephan KE (1997) Useless or helpful? The "limbic system" concept. Rev Neurosci 8(2):139–145

Kwon HG, Hong JH, Jang SH (2010) Mammillothalamic tract in human brain: diffusion tensor tractography study. Neurosci Lett 481(1):51–53. https://doi.org/10.1016/j.neulet.2010.06.052

LeDoux JE (2000) Emotion circuits in the brain. Annu Rev Neurosci 23:155–184. https://doi.org/10.1146/annurev.neuro.23.1.155

Lillethorup TP, Glud AN, Alstrup AKO, Mikkelsen TW, Nielsen EH, Zaer H, Doudet DJ, Brooks DJ, Sorensen JCH, Orlowski D, Landau AM (2018) Nigrostriatal proteasome inhibition impairs dopamine neurotransmission and motor function in minipigs. Exp Neurol 303:142–152. https://doi.org/10.1016/j.expneurol.2018.02.005

Lima LB, Bueno D, Leite F, Souza S, Goncalves L, Furigo IC, Donato J Jr, Metzger M (2017) Afferent and efferent connections of the interpeduncular nucleus with special reference to circuits involving the habenula and raphe nuclei. J Comp Neurol 525(10):2411–2442. https://doi.org/10.1002/cne.24217

Lind NM, Moustgaard A, Jelsing J, Vajta G, Cumming P, Hansen AK (2007) The use of pigs in neuroscience: modeling brain disorders. Neurosci Biobehav Rev 31(5):728–751. https://doi.org/10.1016/j.neubiorev.2007.02.003

Liptrot MG, Sidaros K, Dyrby TB (2014) Addressing the path-length-dependency confound in white matter tract segmentation. PLoS ONE 9(5):e96247. https://doi.org/10.1371/journal.pone.0096247

Maclean PD (1949) Psychosomatic disease and the visceral brain; recent developments bearing on the Papez theory of emotion. Psychosom Med 11(6):338–353

Maclean PD (1952) Some psychiatric implications of physiological studies on frontotemporal portion of limbic system (visceral brain). Electroencephalogr Clin Neurophysiol 4(4):407–418

Mahady LJ, Perez SE, Emerich DF, Wahlberg LU, Mufson EJ (2017) Cholinergic profiles in the Goettingen miniature pig (Sus scrofa domesticus) brain. J Comp Neurol 525(3):553–573. https://doi.org/10.1002/cne.24087

Maier-Hein KH, Neher PF, Houde JC, Cote MA, Garyfallidis E, Zhong J, Chamberland M, Yeh FC, Lin YC, Ji Q, Reddick WE, Glass JO, Chen DQ, Feng Y, Gao C, Wu Y, Ma J, Renjie H, Li Q, Westin CF, Deslauriers-Gauthier S, Gonzalez JOO, Paquette M, St-Jean S, Girard G, Rheault F, Sidhu J, Tax CMW, Guo F, Mesri HY, David S, Froeling M, Heemskerk AM, Leemans A, Bore A, Pinsard B, Bedetti C, Desrosiers M, Brambati S, Doyon J, Sarica A, Vasta R, Cerasa A, Quattrone A, Yeatman J, Khan AR, Hodges W, Alexander S, Romascano D, Barakovic M, Auria A, Esteban O, Lemkaddem A, Thiran JP, Cetingul HE, Odry BL, Mailhe B, Nadar MS, Pizzagalli F, Prasad G, Villalon-Reina JE, Galvis J, Thompson PM, Requejo FS, Laguna PL, Lacerda LM, Barrett R, Dell'Acqua F, Catani M, Petit L, Caruyer E, Daducci A, Dyrby TB, Holland-Letz T, Hilgetag CC, Stieltjes B, Descoteaux M (2017) The challenge of mapping the human connectome based on diffusion tractography. Nat Commun 8(1):1349. https://doi.org/10.1038/s41467-017-01285-x

Mayberg HS (1997) Limbic-cortical dysregulation: a proposed model of depression. J Neuropsychiatry Clin Neurosci 9(3):471–481. https://doi.org/10.1176/jnp.9.3.471

Mayberg HS, Lozano AM, Voon V, McNeely HE, Seminowicz D, Hamani C, Schwalb JM, Kennedy SH (2005) Deep brain stimulation for treatment-resistant depression. Neuron 45(5):651–660. https://doi.org/10.1016/j.neuron.2005.02.014

McIntosh AM, Munoz Maniega S, Lymer GK, McKirdy J, Hall J, Sussmann JE, Bastin ME, Clayden JD, Johnstone EC, Lawrie SM (2008) White matter tractography in bipolar disorder and schizophrenia. Biol Psychiat 64(12):1088–1092. https://doi.org/10.1016/j.biopsych.2008.07.026

Meidahl AC, Orlowski D, Sorensen JC, Bjarkam CR (2016) The retrograde connections and anatomical segregation of the gottingen minipig nucleus accumbens. Front Neuroanat 10:117. https://doi.org/10.3389/fnana.2016.00117

Mufson EJ, Pandya DN (1984) Some observations on the course and composition of the cingulum bundle in the rhesus monkey. J Comp Neurol 225(1):31–43. https://doi.org/10.1002/cne.902250105

Murray EA (2007) The amygdala, reward and emotion. Trends Cognit Sci 11(11):489–497. https://doi.org/10.1016/j.tics.2007.08.013

Nelson AJD, Vann SD (2017) The importance of mammillary body efferents for recency memory: towards a better understanding of diencephalic amnesia. Brain Struct Funct 222(5):2143–2156. https://doi.org/10.1007/s00429-016-1330-x

Orlowski D, Glud AN, Palomero-Galagher N, Sorensen JCH, Bjarkam CR (2019) Online histological atlas of the Gottingen minipig brain. Heliyon 5(3):e01363. https://doi.org/10.1016/j.heliyon.2019.e01363

Orlowski D, Michalis A, Glud AN, Korshoj AR, Fitting LM, Mikkelsen TW, Mercanzini A, Jordan A, Dransart A, Sorensen JCH (2017) Brain tissue reaction to deep brain stimulation—a longitudinal study of DBS in the Goettingen Minipig. Neuromodulation 20(5):417–423. https://doi.org/10.1111/ner.12576

Papez JW (1937) A proposed mechanism of emotion. Arch Neurol Psychiatry 38(4):725–743. https://doi.org/10.1001/archneurpsyc.1937.02260220069003

Pascalau R, Popa Stanila R, Sfrangeu S, Szabo B (2018) Anatomy of the limbic white matter tracts as revealed by fiber dissection and tractography. World Neurosurg 113:e672–e689. https://doi.org/10.1016/j.wneu.2018.02.121

Petersen MV, Lund TE, Sunde N, Frandsen J, Rosendal F, Juul N, Ostergaard K (2017) Probabilistic versus deterministic tractography for delineation of the cortico-subthalamic hyperdirect pathway in patients with Parkinson disease selected for deep brain stimulation. J Neurosurg 126(5):1657–1668. https://doi.org/10.3171/2016.4.jns1624

Seo D, Rabinowitz AG, Douglas RJ, Sinha R (2018) Limbic response to stress linking life trauma and hypothalamus-pituitary-adrenal axis function. Psychoneuroendocrinology 99:38–46. https://doi.org/10.1016/j.psyneuen.2018.08.023

Sorensen JC, Nielsen MS, Rosendal F, Deding D, Ettrup KS, Jensen KN, Jorgensen RL, Glud AN, Meier K, Fitting LM, Moller A, Alstrup AK, Ostergaard L, Bjarkam CR (2011) Development of neuromodulation treatments in a large animal model–do neurosurgeons dream of electric pigs? Prog Brain Res 194:97–103. https://doi.org/10.1016/b978-0-444-53815-4.00014-5

Sturm V, Lenartz D, Koulousakis A, Treuer H, Herholz K, Klein JC, Klosterkotter J (2003) The nucleus accumbens: a target for deep brain stimulation in obsessive-compulsive- and anxiety-disorders. J Chem Neuroanat 26(4):293–299

Swanson LW, Petrovich GD (1998) What is the amygdala? Trends Neurosci 21(8):323–331

Thiebaut de Schotten M, Dell'Acqua F, Valabregue R, Catani M (2012) Monkey to human comparative anatomy of the frontal lobe

association tracts. Cortex 48(1):82–96. https://doi.org/10.1016/j.cortex.2011.10.001

Tournier JD, Calamante F, Connelly A (2007) Robust determination of the fibre orientation distribution in diffusion MRI: non-negativity constrained super-resolved spherical deconvolution. NeuroImage 35(4):1459–1472. https://doi.org/10.1016/j.neuroimage.2007.02.016

Tournier JD, Calamante F, Connelly A (2010) Improved probabilistic streamlines tractography by 2nd order integration over fibre orientation distributions. Proc Int Soc Magn Reson Med 1670

Tournier JD, Calamante F, Connelly A (2012) MRtrix: diffusion tractography in crossing fiber regions. Int J Imaging Syst Technol 22(1):53–66. https://doi.org/10.1002/ima.22005

Tournier JD, Calamante F, Gadian DG, Connelly A (2004) Direct estimation of the fiber orientation density function from diffusion-weighted MRI data using spherical deconvolution. NeuroImage 23(3):1176–1185. https://doi.org/10.1016/j.neuroimage.2004.07.037

Woolf NJ (1991) Cholinergic systems in mammalian brain and spinal cord. Prog Neurobiol 37(6):475–524

Yakovlev PI (1948) Motility, behavior and the brain; stereodynamic organization and neural coordinates of behavior. J Nerv Ment Dis 107(4):313–335